



Biomarker and Carbon Isotope Composition of the Oil Stains from the North Hadramaut High Area of Eastern Yemen: Implications on the Nature of Organic Matter Input and Their Characteristics

Mohammed Hail Hakimi¹ · Abbas F. Gharib² · Nor Syazwani Z. Abidin³ · Adeeb Ahmed⁴ · Mohamed M. El Nady⁵ · Madyan M. A. Yahya¹ · Aref A. Lashin⁶

Received: 19 January 2021 / Accepted: 22 May 2021 / Published online: 23 June 2021
© King Fahd University of Petroleum & Minerals 2021

Abstract

Five core sandstone and carbonate rock samples from the Cretaceous Harshiyat Formation containing oil stains were collected from two wells in the North Hadramaut High area (eastern Yemen) and geochemically analyzed by their sterane and terpane biomarker and stable carbon isotope ($\delta^{13}\text{C}$) compositions. This paper studied the geochemical characteristics of the oil stains and their relation to probable potential source rocks. The source rock characteristics include the origin of organic matter input; redox depositional conditions, lithology, and degree of thermal maturity were investigated. The saturated and aromatic hydrocarbon fractions of the analyzed oil stain samples have $\delta^{13}\text{C}$ values in the range of -26.5‰ – -28.6‰ and -26.3‰ – -26.7‰ , respectively. These $\delta^{13}\text{C}$ values indicate that the oil stain samples originated from a mixed organic matter input in their source rock. The presence of mixed marine and terrestrial organic matter in the source rock is further concluded from biomarker distributions of *n*-alkane, isoprenoid, terpane, and sterane. These biomarkers and their ratio parameters suggest that the analyzed oil stain samples were sourced from clay-rich rock deposited in marine-reducing environmental conditions and likely contained mixed planktonic/bacterial organic matter and land plant inputs. Both saturated and aromatic maturity biomarkers suggest that the analyzed oil stains were from a mature source rock, equivalent to a moderate to peak-mature oil window. The environmental biomarker indicators of the studied oil stain samples correlated well with the shales in the Late Cretaceous Harshiyat Formation in the onshore Jiza-Qamar Basin (eastern Yemen), indicating that the analyzed oil stains were generated from a mature Harshiyat source rock in the onshore Jiza-Qamar Basin and subsequently migrated into the Cretaceous Harshiyat sandstone and limestone reservoirs in the North Hadramaut High area (eastern Yemen) through normal faults system.

Keywords Harshiyat Formation · North Hadramaut high · Eastern Yemen · Oil stain · Biomarker · Carbon isotope · Geochemical correlation

✉ Mohammed Hail Hakimi
ibnalhakimi@yahoo.com

¹ Geology Department, Faculty of Applied Science, Taiz University, 6803 Taiz, Yemen

² Oil and Gas Economics, Imam Jaafar Al-Sadiq University, Kirkuk, Iraq

³ Geosciences Department, Faculty of Science and Information Technology, Universiti Teknologi PETRONAS, 32610 Bandar Seri Iskandar, Perak, Malaysia

⁴ Department of Earth and Environmental Sciences, Bahria University, Islamabad 44000, Pakistan

⁵ Exploration Department, Egyptian Petroleum Research Institute, Nasr City, Cairo 11727, Egypt

⁶ Petroleum and Natural Gas Engineering Department, College of Engineering, King Saud University, P.O. Box 800, Riyadh 11421, Saudi Arabia



1 Introduction

The area of interest of this study is the North Hadramaut High area, belonging to the Hadramaut government in eastern Yemen (Fig. 1a). The North Hadramaut High is a regional subsurface high and separates the Masila and Jiza-Qamar Basins in the south and Rub' Al-Khali Basin in the north (Fig. 1a). To date, the North Hadramaut High represents a grossly underexplored area, where limited exploration wells have been drilled by multiple oil companies (Fig. 1b). Oil stain samples were discovered in the clastic and carbonate rocks of the Late Cretaceous Harshiyat Formation encountered in two exploration wells (Thamoud-01 and Tarfayt-02), as shown in Fig. 1b.

The Cretaceous sedimentary rocks in the North Hadramaut High area are mainly marine and subordinate continental sediments composed of sandstone, carbonate, and shales (Fig. 2). Sandstone and carbonate rocks of Qishn and Harshiyat Formations (Fig. 2) can be considered as reservoir rocks in the North Hadramaut High area. The shale intervals in the Harshiyat Formation are considered as good potential source rocks in the onshore and offshore of basins of the Yemen [1, 2]. The Harshiyat shales are deposited in a marine environment under low oxygen conditions and contain mixed organic matter with types I, II, and III kerogens, consistent with both oil and gas source rocks [1, 2]. Hence, exploration activities for conventional petroleum resources have been intensively focused on organic-rich shale intervals within the Late Cretaceous Harshiyat Formation.

In this study, five oil stain samples, extracted from the sandstone and carbonate rocks of the Late Cretaceous Harshiyat Formation obtained in two well locations (Thamoud-01 and Tarfayt-02) in the North Hadramaut High area (Fig. 1b), were geochemically analyzed. We used the oil composition of the analyzed oil stain samples to document the characteristics of the potential source rock, such as the origin of the source organic matter input, paleodepositional conditions, lithology, and thermal maturity. This study subsequently incorporated biomarker and $\delta^{13}\text{C}$ results, which are best used to provide dependable geochemical interpretations and understand the genetic relationships between the oil stains under study and the Harshiyat source rock.

2 Stratigraphic Setting

The stratigraphic column of the North Hadramaut High area includes a Precambrian basement rock and a sedimentary succession ranging in age from Paleozoic to Tertiary (Fig. 2). The lower Palaeozoic sedimentary sequence is represented by the Wajid and Akbra formations that lie unconformably on Precambrian basement rock (Fig. 2). The Wajid Formation is characterized by continental sandstones and interbedded mudstones from the Cambrian–Carboniferous age, while the Akbra Formation represents glacial deposits from the Permian ice age [3, 4].

The Mesozoic section is dominated by thick clastic and carbonate rocks, forming the Kuhlan Formation and Amran (Jurassic) and Mahara (Cretaceous) Groups (Fig. 2). The Early–Middle Jurassic Kuhlan Formation is represented

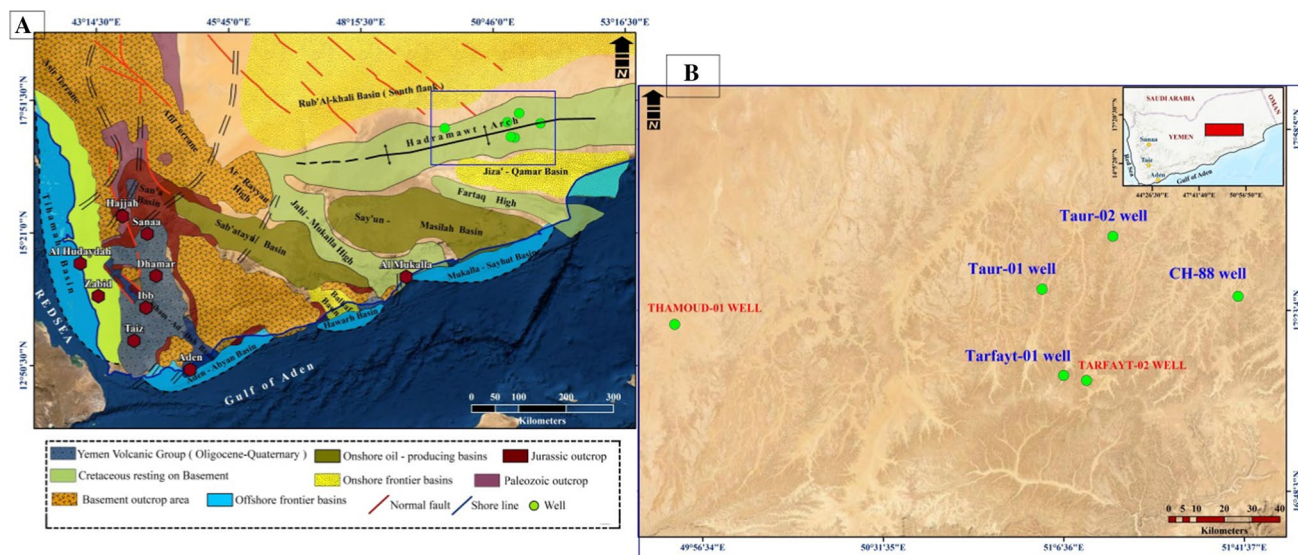


Fig. 1 a Map showing the locations of the sedimentary basins in Yemen, including the North Hadramaut High area of eastern Yemen (after Hakimi et al., 2020). b Location map of the exploration wells in

the North Hadramaut High area, including the locations of the studied wells (i.e., Thamoud-01 and Tarfayt-02)

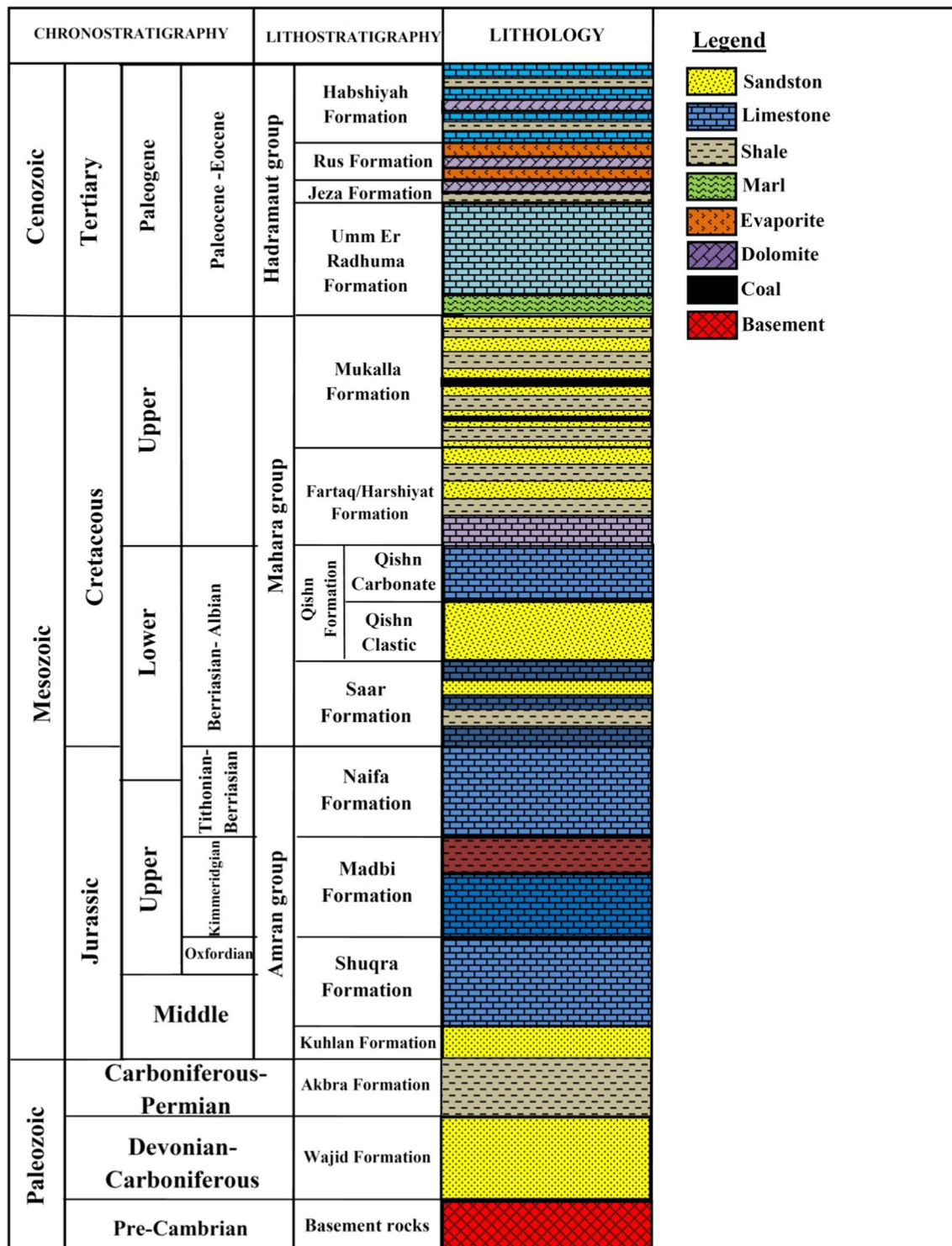


Fig. 2 Generalized stratigraphic column of the Cretaceous–lowermost Paleogene succession in the North Hadramaut High area of eastern Yemen. Oil stain samples for this study were taken from clastic and carbonate rocks in the Harshiyat Formation

by continental to marine sandstones which vertically grade upward into the carbonates of the Amran Group [3]. Here, Jurassic deposits of Amran Group were accumulated during Jurassic period and contain three sedimentary formations,

from base to top, namely the Shuqra Formation, the Madbi Formation, and the Naifa Formation (Fig. 2). The Amran Group was followed by the mixed clastics and carbonates of the Mahara Group (Fig. 2). The Mahara Group was divided

into four formations from base to top: Saar, Qishn, Harshiyat/Fartaq, and Mukalla formations (Fig. 2). In the North Hadramaut High, the Lower Cretaceous Qishn Formation lies on Amran Group with a conformable contact (Fig. 2). The clastic rocks of the Qishn Formation are considered as the main reservoir rocks in most oilfields of Masila Basin in eastern Yemen [5–7].

The Qishn Formation is overlain conformably by the Upper Cretaceous Harshiyat Formation (Fig. 2), which extends into the offshore Masila and Jiza-Qamar Basins [4]. The Harshiyat Formation consists of sandstones and interbedded shales deposited in shallow-marine settings [1, 3] with vertical variations in lateral carbonate facies for the Fartaq Formation (Fig. 2). The Harshiyat shales are considered as potential source rocks for both oil and gas hydrocarbons in the onshore and offshore basins of Yemen [1, 2]. The Upper Cretaceous Harshiyat Formation is followed by deltaic sediments of the Mukalla Formation (Fig. 2). The Mukalla Formation has been assigned to the Santonian–early Campanian as indicated from calcareous nannofossils [8] and composed of non-marine sandstones and intercalated with carbonaceous shales and coal beds (Fig. 2). The carbonaceous shale and coal sediments of the Mukalla Formation are considered as deltaic source rocks in the Jiza-Qamar Basin [9], consistent with Type II/III kerogens [10, 11].

The North Hadramaut High is filled with Tertiary (Paleocene-Eocene) succession (Fig. 2). During the Late Paleocene, the transgressive shales of the Umm Er Radhuma Formation were deposited because of sea-level rise. The Umm Er Radhuma shales contain a mixture of aquatic organic matter (planktonic and bacterial) and terrigenous organic matter and deposited under anoxic marine conditions as indicated by biological marks of the organic matter [12]. However, the Umm Er Radhuma Formation is also composed of thick carbonate rocks at the top (Fig. 2), and this carbonate lithology confirmed a marine environment setting [3, 12]. The Umm Er Radhuma Formation continued to the Early Eocene and was followed by mixed carbonate, clastics and anhydrite deposits of the Jiza, Rus, and Habshiyah Formations (Fig. 2).

3 Samples and Methods

Five core sandstone and carbonate samples containing oil stains were collected from the Thamoud-01 and Tarfayt-02 wells in the North Hadramaut High area (Table 1; Fig. 1b). Oil stains have been reported from the Harshiyat Formation at 723, 1218 (limestone rocks), and 1212 m (Sandstone rocks) in the Tarfayt-02 well (Table 1) and at 449 and 479 m (Sandstone rocks) in the Thamoud-01 well (Table 1).

The selected sandstone and carbonate cores containing oil stains were finely milled (60 μm) and subjected to organic

geochemical analyses, including gas chromatography, gas chromatography–mass spectrometry (GC–MS), and mass spectrometry for $\delta^{13}\text{C}$. Most organic geochemical analyses were conducted at Simon Petroleum Technology Limited Laboratories, UK, and the results are made available through the Petroleum Exploration and Production Authority (PEPA) of Republic of Yemen.

The oil stains were extracted from the sandstone and carbonate samples using a standard extraction process by a mixture solvent of dichloromethane (DCM) and methanol (CH_3OH) for 72 h. The extracted materials were separated into hydrocarbon (saturate and aromatic) and non-hydrocarbon (polar) fractions using a long liquid column chromatography on silica gel topped with alumina oxide.

The saturated fraction of the five oil stain samples was analyzed using the flame ionization detector (FID) of a gas chromatograph with an AMS-92 column. The furnace temperature of the GC oven was programmed between 70 $^\circ\text{C}$ and 270 $^\circ\text{C}$ at a rate of 3 $^\circ\text{C}/\text{min}$ and held at 290 $^\circ\text{C}$ for 20 min. Of these samples, three saturated and two aromatic fractions were subjected to GC–MS analysis. The GC–MS experiment was performed on a Finnegan 4000 mass spectrometer using a gas chromatograph attached directly to the ion source with the temperature programmed from 60 $^\circ\text{C}$ to 300 $^\circ\text{C}$ at a rate of 3 $^\circ\text{C}/\text{min}$ and then held for 20 min at 300 $^\circ\text{C}$. GC–MS analysis was used to deduct the biological marks of organisms in the saturated and aromatic hydrocarbon fractions using specific ions such as m/z 191, m/z 217, m/z 178, m/z 184, m/z 192, and m/z 198 mass fragmentograms. The peak assignments of the specific ions (Table 2) were identified by comparison of the retention times and mass spectra of the monitored ions with previous works [13–16].

Additionally, saturated and aromatic fractions of two extracted oil stain samples were analyzed for bulk $\delta^{13}\text{C}$ compositions. $\delta^{13}\text{C}$ values were measured using a VG 602 stable isotope mass spectrometry instrument following the standard procedure of the Simon Petroleum Technology Limited Laboratories, UK. The $^{13}\text{C}/^{12}\text{C}$ isotope ratio of CO_2 from a sample was compared with the corresponding ratio of a reference (NBS22 standard) and calibrated against the PDB standard.

4 Results and Discussion

4.1 Biomarker Distributions

4.1.1 Lipid Biomarker Fingerprints

Lipid biomarkers (e.g., *n*-alkanes, acyclic isoprenoids, triterpanes, and steranes) in the saturated hydrocarbon fraction of the five oil stain samples obtained from the gas chromatogram and fragmentograms of m/z 191 and m/z 217 ions

Table 1 Specific biomarker ratios and carbon isotopes of saturated and aromatic hydrocarbon fractions in the oil staining samples from the clastic and carbonate rocks in Harshiyat Formation, North Hadramaut High of eastern Yemen, illustrating source organic matter and depositional environment conditions and thermal maturity degree of their source rock

Wells	Depth (m)	Lipids and aromatic biomarkers														Carbon isopods (%)											
		Source organic matter and depositional environment conditions																									
		Pr/Ph	Ph/C ₁₈	Ph/C ₁₇	CPI	C ₂₉ /C ₃₀	Ts/Tm	HCR ₃₁ /HC ₃₀	Tricyclic terpanes	DBT/Phen	C ₂₇ /C ₂₉	Regu- lar ster- anes	Regular steranes (%)	C ₃₂ 22S/ (22S + 22R)	C ₂₉ 20S/ (20S + 20R)		C ₂₉ ββ/ (ββ + αα)	M ₃₀ /C ₃₀	MPI-1	MPI-2	MDR	VRC	Satu- rated	Aro- matic			
Tham-oud-01	Sand- stone	449	0.60	0.73	0.79	1.22	0.77	0.48	0.31	0.69	2.37	2.14	0.36	0.94	37.7	22.2	40.1	0.61	0.43	0.55	0.13	0.72	0.89	4.19	0.83	-26.5	-26.3
	Sand- stone	479	0.65	0.61	0.73	1.29	0.68	0.93	0.27	0.65	2.67	3.12	-	1.52	46.1	23.5	30.4	0.62	0.42	0.55	0.14	-	-	-	-	-	-
Tar-fayt-02	Lime- stone	723	0.98	0.72	0.66	1.41	-	-	-	-	-	-	-	-	-	-	-	-	-	-	-	-	-	-	-	-	-
	Sand- stone	1212	0.77	0.58	0.52	1.17	-	-	-	-	-	-	-	-	-	-	-	-	-	-	-	-	-	-	-	-	-
	Lime- stone	1218	0.99	0.50	0.48	1.07	0.64	0.63	0.42	0.68	3.38	1.76	0.23	0.80	34.4	22.8	42.8	0.57	0.48	0.57	0.14	0.82	1.02	1.80	0.89	-28.6	-26.7

Pr—pristane, Ts—(C₂₇ 18α (H)-22, 29, 30-trisnorhopane), CPI—carbon preference index (1): (2(C₂₃ + C₂₅ + C₂₇ + C₂₉) / (C₂₂ + 2[C₂₄ + C₂₆ + C₂₈] + C₃₀)), Ph—phytane, Tm—(C₂₇ 17α (H)-22, 29, 30-trisnorhopane), HCR₃₁/HC₃₀: C₃₁ regular homohopane/C₃₀ hopane, C₂₉/C₃₀: C₂₉ norhopane/C₃₀ hopane, M₃₀/C₃₀: C₃₀ moretane/C₃₀ hopane, DB = dibenzothiophene, Phen = phenanthrene, MDR = 4-MDBT/1-MDBT, MPI-1: methylphenanthrene index = 1.5 × (2-MP + 3-MP) / (phenanthrene + 1 - MP + 9-MP), MPI-2: methylphenanthrene index = 3 × (2-MP / (phenanthrene + 1 - MP + 9-MP). VRC (%) = 0.60 * MPI-1 + 0.40

Table 2 Peak assignments for hydrocarbons in the saturated fractions in the m/z 191 (I) and 217 (II) mass fragmentograms

Compound abbreviation		
(I) Peak no		
Ts	18 α (H),22,29,30-trisnorhopane	Ts
Tm	17 α (H),22,29,30-trisnorhopane	Tm
29	17 α ,21 β (H)-norhopane	C ₂₉ hop
30	17 α ,21 β (H)-hopane	Hopane
29 M	17 β (H),21 α (H)-hopane (moretane)	C ₂₉ Mor
30 M	17 β ,21 α (H)-moretane	C ₃₀ Mor
31S	17 α ,21 β (H)-homohopane (22S)	C ₃₁ (22S)
31R	17 α ,21 β (H)-homohopane (22R)	C ₃₁ (22R)
32S	17 α ,21 β (H)-homohopane (22S)	C ₃₂ (22S)
32R	17 α ,21 β (H)-homohopane (22R)	C ₃₂ (22R)
33S	17 α ,21 β (H)-homohopane (22S)	C ₃₃ (22S)
33R	17 α ,21 β (H)-homohopane (22R)	C ₃₃ (22R)
34S	17 α ,21 β (H)-homohopane (22S)	C ₃₄ (22S)
34R	17 α ,21 β (H)-homohopane (22R)	C ₃₄ (22R)
35S	17 α ,21 β (H)-homohopane (22S)	C ₃₅ (22S)
35R	17 α ,21 β (H)-homohopane (22R)	C ₃₅ (22R)
(II) Peak no		
a	13 β ,17 α (H)-diasteranes 20S	Diasteranes
b	13 β ,17 α (H)-diasteranes 20R	Diasteranes
c	13 α ,17 β (H)-diasteranes 20S	Diasteranes
d	13 α ,17 β (H)-diasteranes 20R	Diasteranes
e	5 α ,14 α (H), 17 α (H)-steranes 20S	$\alpha\alpha$ 20S
f	5 α ,14 β (H), 17 β (H)-steranes 20R	$\alpha\beta$ 20R
g	5 α ,14 β (H), 17 β (H)-steranes 20S	$\alpha\beta$ 20S
h	5 α ,14 α (H), 17 α (H)-steranes 20R	$\alpha\alpha$ 20R

are presented in Figs. 3 and 4, and the summary of the compound ratios is listed in Table 1.

The n -alkane distributions are mainly between the n -C₁₆ to the n -C₃₆ of the studied oil stain samples, as shown in the gas chromatograms (Fig. 3). Among these distributions of n -alkane, even normal alkanes prevail over odd n -alkanes, with the highest abundance of n -C₁₇ to n -C₂₃ compounds (Fig. 3). These distributions result in carbon preference index (CPI) values between 1.07 and 1.41 (Table 1).

Acyclic isoprenoids such as pristane (Pr) and phytane (Ph) are also present in all analyzed samples (Fig. 3), derived from the chlorophyll phytol chain. Pr and Ph occurred in low concentrations in most analyzed oil stain samples (Fig. 3). The ratio of Pr/Ph is less than 1, between 0.60 and 0.99 (Table 1), representing the Ph is higher than Pr (Fig. 3). However, normal n -C₁₇ and n -C₁₈ alkanes are very often associated with these isoprenoids [15, 17]. The isoprenoid ratios relative to the n -alkane concentrations (Pr/ n -C₁₇ and Ph/ n -C₁₈) were subsequently calculated and found to be in the ranges of 0.50–0.73 and 0.48–0.79, respectively (Table 1). These findings represent that the concentrations

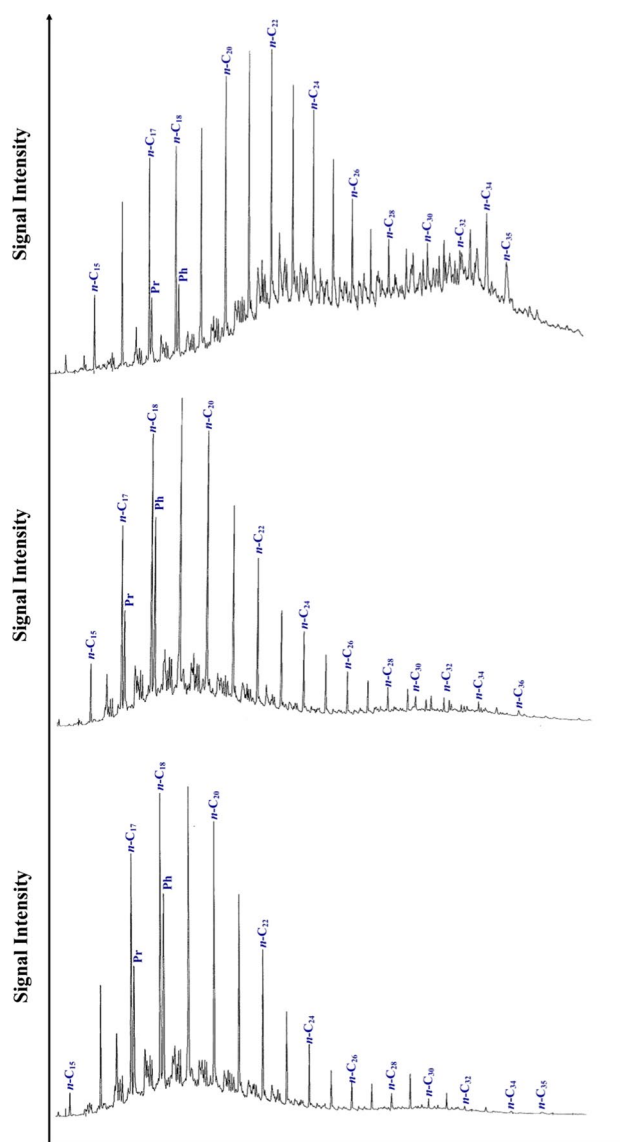


Fig. 3 Gas chromatograms of the saturated hydrocarbon fraction for three oil stain samples analyzed, showing a complete suite of acyclic isoprenoids (e.g., pristane and phytane) and low-molecular-weight n -alkanes, indicating that there is no biodegradation in the analyzed samples

of n -alkane (n -C₁₇ and n -C₁₈) were higher than those of Pr and Ph isoprenoids in all examined oil stain samples (Fig. 3).

The GC–MS mass fragmentograms of the m/z 191 and m/z 217 ions of three oil stain samples analyzed affirmed the presence of hopanoids and steroids in the saturated hydrocarbon fraction (Fig. 4).

The mass fragmentograms of the m/z 191 chromatograms show significant amounts of hopanes over tricyclic terpanes, predominated by C₃₀-hopane, C₂₉-norhopane, and C₃₁–C₃₃ homohopanes (Fig. 4a). Among these, C₃₀-hopane was observed in high abundance compared with C₂₉-norhopane, leading to low C₂₉/C₃₀ hopane

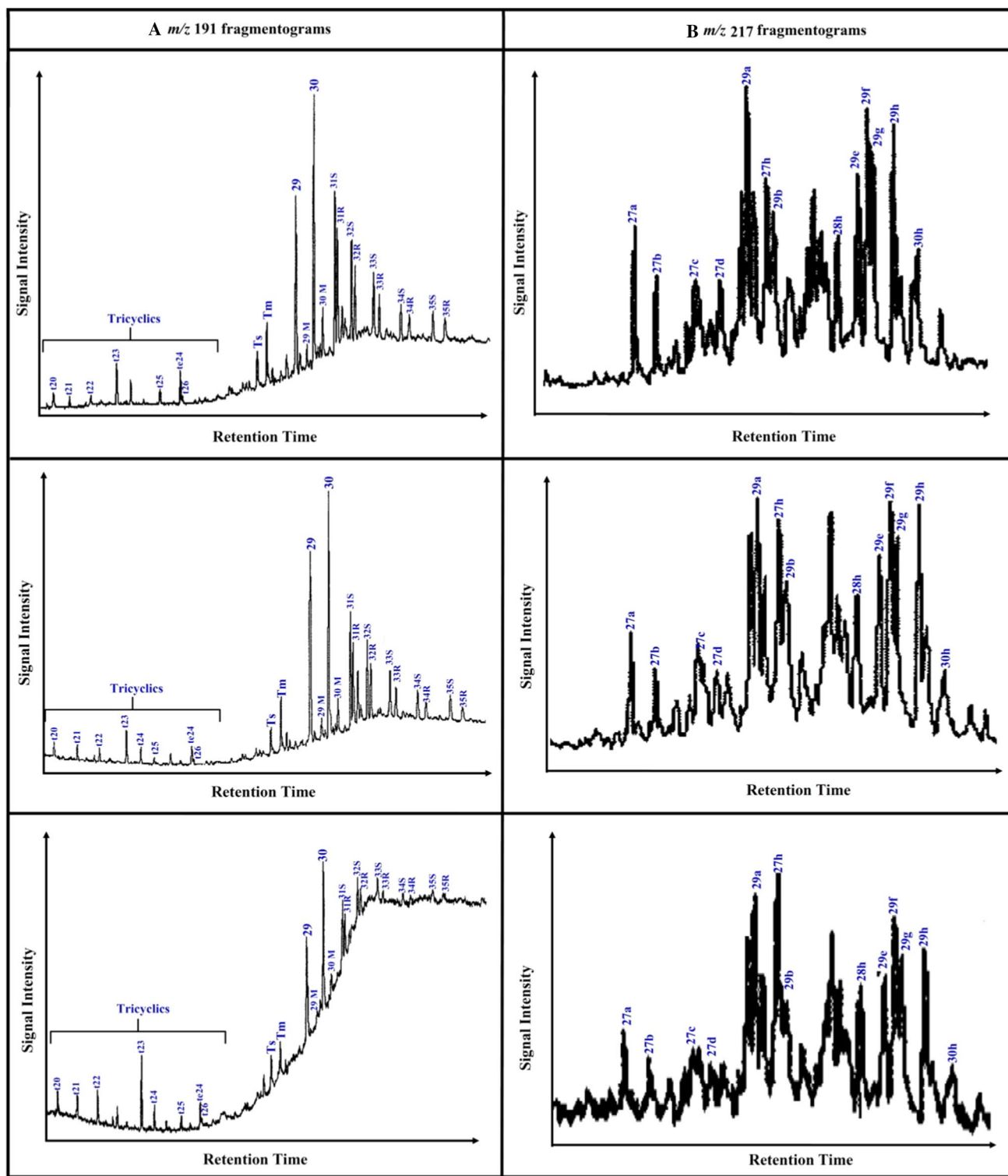


Fig. 4 Mass fragmentograms of the m/z 191 and m/z 217 ions of the saturated hydrocarbon fraction for two analyzed oil stain samples. The biomarkers shown in this Figs. a and b are identified in Table 2

values of less than 1 (0.64–0.77; Table 1) and hinting at a typical clay-rich source rock [18]. The C_{31} – C_{35} homohopanes from the examined oil stain samples were observed

in decreasing quantities from C_{31} to C_{35} (Fig. 4a). Meanwhile, the C_{31} 22R-series homohopanes were less abundant than the C_{30} -hopane (Fig. 4a), as evidenced by the low C_{31}

22R homohopane/ C_{30} -hopane ($C_{31}R/C_{30}H$) ratios between 0.27 and 0.42 (see Table 1). The analyzed oil stains also display a low concentration of 17 α (H)-trisorneohopane (Tm) and 18 α (H)-trisorneohopane (Ts), with Tm concentration slightly higher than that of Ts (Fig. 4a), leading to relatively low values of Ts/Tm (less than 1.0; Table 1). The biomarker maturity ratios of C_{32} 22S/(22R + 22S) and moretane to hopane ($C_{30}M/C_{30}H$) of the analyzed oil stain samples were subsequently calculated (Table 1). Moreover, the low amounts of tricyclic terpanes (C_{20} – C_{26}) were also recorded in the m/z 191 mass fragmentogram of the analyzed samples (Fig. 4a), and the ratios of tetracyclic and tricyclic terpanes such as $C_{23}T/C_{24}T$, $C_{26}T/C_{25}T$, and $TeC_{24}/C_{26}T$ were subsequently calculated (Table 1).

Biomarker distributions of regular sterane and diasteranes in three oil stain samples analyzed were also observed in the saturated hydrocarbon fraction and identified from m/z 217 chromatograms in Fig. 4b. The mass fragmentograms of m/z 217 chromatograms are characterized by the high abundance of steranes compared with diasterane biomarkers (Fig. 4b). In addition, the relative percentages of the regular C_{27} , C_{28} , and C_{29} steranes and source ratios of the regular C_{27}/C_{29} steranes and C_{29} maturity ratios of $20S/(20S + 20R)$ and $\alpha\beta\beta$ ($\alpha\beta\beta + \alpha\alpha\alpha$) are calculated from the sterane distributions (Fig. 4b) and are also reported in Table 1. The results indicate higher quantities of the C_{27} and C_{29} regular steranes than the C_{28} regular steranes (Fig. 4b), with a high proportion of C_{27} (34.4%–46.1%) and C_{29} (30.4%–42.8%) compared with C_{28} (22.2%–23.5%) as shown in Table 1.

4.1.2 Aromatic Biomarkers

Aromatic biomarkers are more abundant in terrestrial plants in general and are useful indicators of thermal maturity [19–21], depositional environment and lithologies [22], and source facies [23, 24]. In this study, polycyclic aromatic biomarkers such as dibenzothiophene (DBT), phenanthrene (P), alkylnaphthalene, and methylphenanthrene and their ratios and parameters were identified in the aromatic hydrocarbon fraction of two investigated oil stain samples. The relative aromatic distributions of DBF, P, and the homologs of methyl-dibenzothiophene and methylphenanthrene were obtained from the mass fragmentograms of m/z 184, m/z 178, m/z 192, and m/z 198, respectively.

Most ratios of methylphenanthrene (MPI-1 and MPI-2), methyl-dibenzothiophene (MDR), and dibenzothiophene/phenanthrene (DBT/P) were calculated on the basis of isomer distribution of aromatic compounds (see Table 1). The calculated reflectance (VRc) was subsequently determined on the basis of the methylphenanthrene index (MPI-1) [25].

4.2 Bulk $\delta^{13}C$ Compositions

Bulk $\delta^{13}C$ of the saturated and aromatic portions of the oil composition is frequently used to categorize crude oils and determine the origins of organic matter input in possible source rocks [26–29]. The $\delta^{13}C$ values of these hydrocarbon portions are also used to distinguish between the proportions of terrigenous and marine organic matter inputs [28–30]. According to Sofer [28], terrigenous sourced oils have $\delta^{13}C$ aromatic hydrocarbon values ranging from -25% to -32% , whereas marine origin oils have $\delta^{13}C$ saturated hydrocarbon values between -25% and -33% .

In this study, bulk stable $\delta^{13}C$ analyses were performed on the derivative saturated and aromatic hydrocarbon fractions of the two analyzed oil stains, as shown in Table 1. The saturated and aromatic hydrocarbon fractions have $\delta^{13}C$ values in the range of -26.5% to -28.6% and -26.3% to -26.7% , respectively. These values of saturated ($\delta^{13}C_{Sat.}$) and aromatic ($\delta^{13}C_{Aro.}$) isotopic compositions were plotted on a Sofer [28] diagram and showed that the analyzed oil stain samples originated from a single source rock and that this source rock received a mixed marine and terrigenous organic matter input (Fig. 5a). These $\delta^{13}C$ values of the analyzed oil stain samples are similar to those of the organic matter-rich shale intervals of the Late Cretaceous Harshiyat source rock (Fig. 5a) as indicated by the recent work of Hakimi et al. [2].

In addition, $\delta^{13}C$ fraction data were used to give information on the deposition age of the probable source rocks. The geologic time of deposition was estimated on the basis of the $\delta^{13}C$ values of the saturated fraction [31]. In this respect, the analyzed oil stain samples have saturated ($\delta^{13}C_{Sat.}$) isotopic values between -26.5% and -28.6% (Table 1) and this range of the saturated isotopic ($\delta^{13}C_{Sat.}$) suggests that the probable source rock of the analyzed oil stain samples was generally deposited during the Cretaceous time, as demonstrated from diagram of saturated ($\delta^{13}C_{Sat.}$) isotopic values adjacent to geological ages (Fig. 5b). This finding further suggests that there is a genetic link between the analyzed oil stain samples and the Late Cretaceous Harshiyat source rock.

4.3 Organic Matter Characteristics and the Sedimentary Conditions of the Source Rock

In this study, on the basis of saturated and aromatic biomarker results described in the previous paragraphs, the characteristics of the probable source rock such as organic matter input, lithology, and sedimentary environmental conditions and the degree of thermal maturation were established and assessed [2, 14, 15, 32, 33].

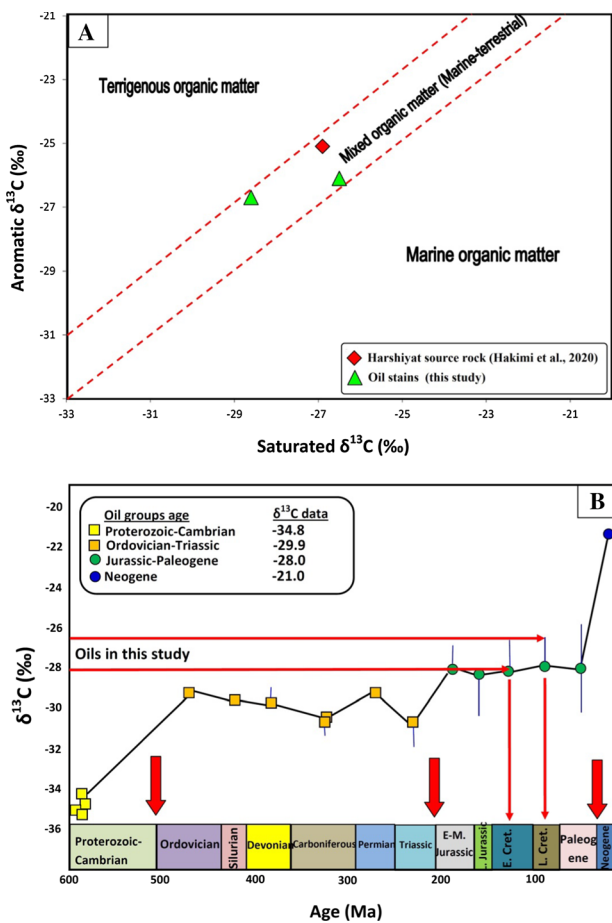


Fig. 5 **a** A Sofer plot of $\delta^{13}C_{aro}$ versus $\delta^{13}C_{sat}$ for the analyzed oil stains samples. The dotted line represents the best-fit separation for waxy and non-waxy oils and is described by the equation $\delta^{13}C_{aro} = 1.14 \delta^{13}C_{sat} + 5.46$, following Sofer (1984). **b** Carbon isotope source age assignment, suggesting a Cretaceous age affinity for the analyzed oil stain samples (modified after Andrushevich et al., 1998)

The results of the lipid biomarkers in the saturated hydrocarbon fraction of the analyzed oil stain samples imply that the probable source rock is a clay-rich facies deposited in a marine environment under suboxic conditions, containing mixed marine and terrestrial organic matters.

In most of the analyzed samples, normal alkanes show the highest abundance of short- to middle-chain *n*-alkanes and small amounts of long-chain *n*-alkane (Fig. 3), suggesting typical oils derived from marine organic matter mixed with terrigenous organic input [34–36]. These findings are also consistent with the isoprenoid ratios of Pr/Ph, Pr/*n*-C₁₇, and Ph/*n*-C₁₈ and from CPI values (Table 1). The relatively high concentrations of Ph (Fig. 3) with low Pr/Ph, Pr/*n*-C₁₇, and Ph/*n*-C₁₈ ratios (Table 1) indicate that the analyzed oil stain samples sourced from sediments contain mixed organic matter of marine and terrigenous origins and are deposited under reductive conditions (Fig. 6). The interference of the

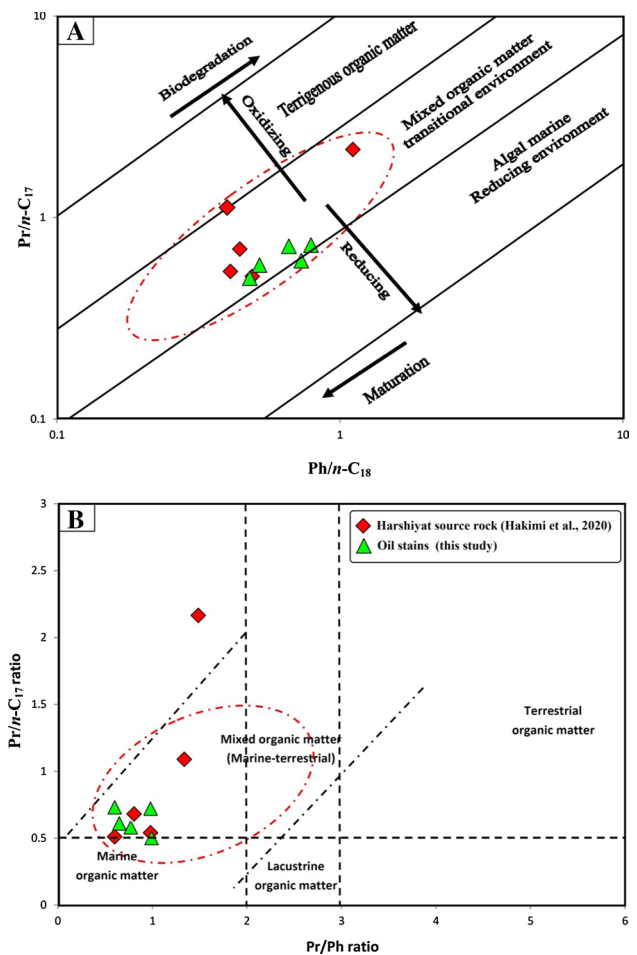


Fig. 6 Geochemical biomarker results of the analyzed oil stain samples and Harshiyat source rock from a recent work of Hakimi et al. (2020). **a** Pristane/*n*-C₁₇ versus phytane/*n*-C₁₈ (from Shanmugam, 1985) and **b** pristane/phytane versus pristane/*n*-C₁₇, providing a novel, convenient, and powerful way to infer a good oil–source rock geochemical correlation

organic matter input is also in line with the CPI values [15]. Data show that the CPI values of 90% of the samples are less than 1.3, whereas the values for the remaining 10% are greater than 1.3 (Table 1), further indicating mixed marine and terrestrial plant organic matter (Fig. 7). The presence of plant organic matter in the source rock is also deduced from the relatively high proportions of Tm compared with Ts in the aliphatic hydrocarbon fraction of the analyzed oil stain sample (Fig. 4b), as the relative abundance of Tm is indicative of organic matter derived from land plants [37, 38].

In this study, tricyclic terpene (*m/z* 191) distributions were also diagnostic of organic matter and paleodepositional environments [15, 39–44]. The greater quantities of the C₂₅ tricyclic terpene in contrast to that of C₂₆ tricyclic in the analyzed oil stain samples (Fig. 4a) indicate a marine depositional environment of their probable source rock. The cross-plot of C₂₆T/C₂₅T tricyclic terpanes against the C₃₁

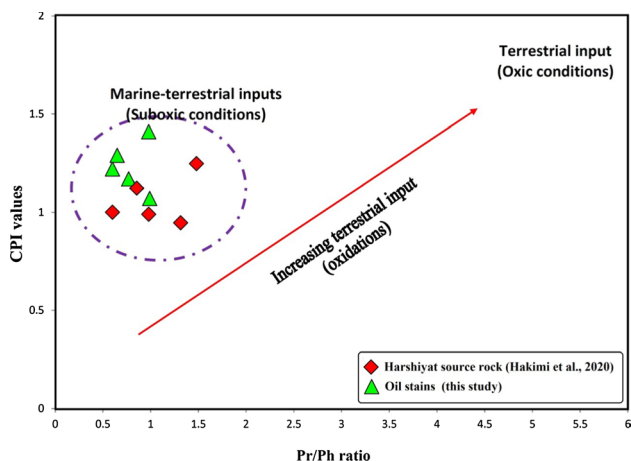


Fig. 7 Geochemical biomarker ratios of pristane/phytane and CPIs in the analyzed oil stain samples and Harshiyat source rock from a recent work of Hakimi et al. (2020), showing mixed organic matter of marine and terrestrial organic matter and inferring a good oil–source rock geochemical correlation

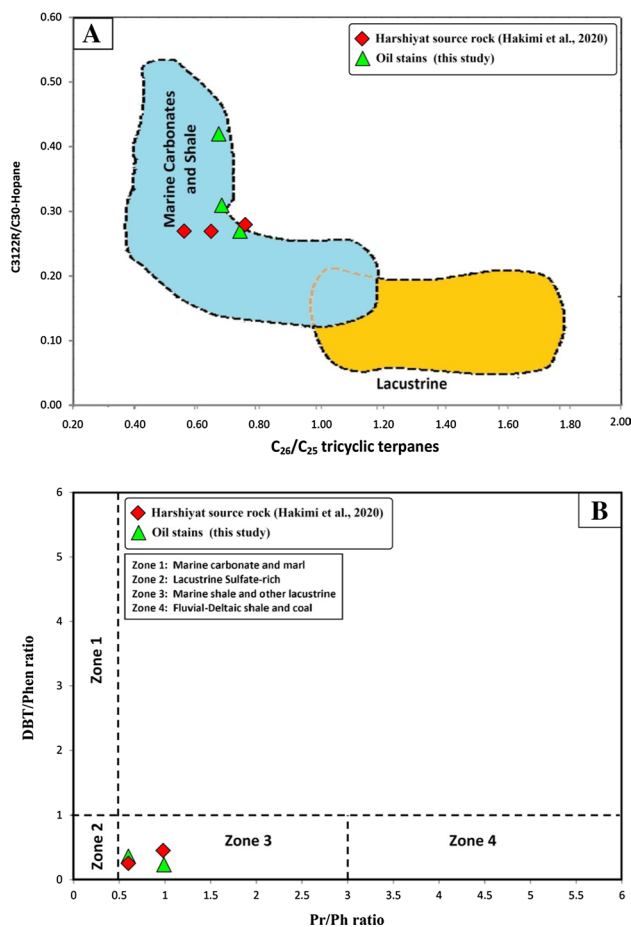


Fig. 8 Cross-plots of the C_{26}/C_{25} tricyclic terpane ratio versus $C_{31}R/C_{30}$ hopane and ratios of pristane/phytane versus DBT/Phen for the analyzed oil stain samples and Harshiyat source rock from a recent work of Hakimi et al. (2020), implying a clay-rich marine source rock

22R homohopane/ C_{30} -hopane ($C_{31}R/C_{30}H$) ratio in Fig. 8a reinforces the idea of a marine source rock. In addition, the low Pr/Ph and DBT/Phen ratios less than 1 indicate that the analyzed oil stain samples were sourced from a marine clay-rich rock (Fig. 8b). The high $C_{23}T/C_{24}T$ ratio is compatible with the relatively high $C_{24}Te/C_{26}T$ ratio (Table 1), further suggesting a source rock containing mixed marine and terrestrial organic matter and deposited in suboxic environmental conditions (Fig. 9).

The abundance of C_{27} and C_{29} regular steranes in the saturated hydrocarbon fraction of the analyzed oil stain samples (Fig. 4b; Table 1) further suggests a contribution of mixed marine planktonic/algae and terrestrial land plants to the source rock. This was observed from the plot of the concentrations of the C_{27} , C_{28} to C_{29} regular steranes on a Huang and Meinschein [45] adapted ternary diagram (Fig. 10) and the C_{27}/C_{28} regular sterane ratio of the oil stain samples under study (Table 1; Fig. 11). A mixed organic matter input in the source rock is further emphasized by the bulk $\delta^{13}C$ data of the saturated and aromatic hydrocarbon fractions (Fig. 5a).

4.4 Thermal Maturity of the Source Rock

In this study, the degree of thermal maturity of the oil stain samples and their probable source rock was assessed from representative aliphatic sterane and hopane biomarker ratios and parameters of the aromatic hydrocarbon fractions in the analyzed oil stain samples, as shown in Table 1.

The isomerization ratios of 22S/ (22S + 22R) C_{32} hopanes, 20S/ (20S + 20R) and $\beta\beta/$ ($\beta\beta + \alpha\alpha$) C_{29} steranes, followed by slower reactions such M_{30}/C_{30} , Ts/Tm

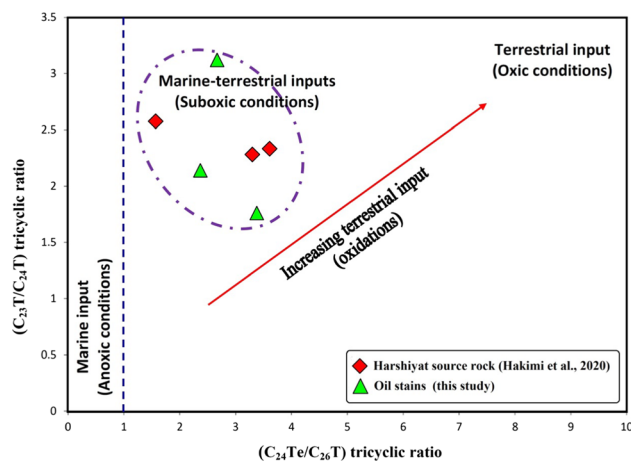


Fig. 9 Geochemical biomarker results of the $C_{23}T/C_{24}T$ and $C_{24}Te/C_{26}T$ tricyclic ratios for the analyzed oil stain samples and Harshiyat source rock from a recent work of Hakimi et al. (2020), showing mixed marine and terrestrial organic matter deposited under suboxic conditions

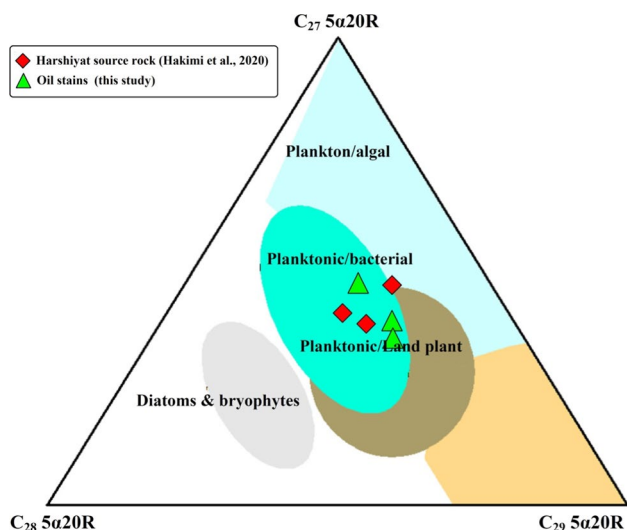


Fig. 10 Ternary diagram of regular steranes (C_{27} – C_{29}) of the analyzed oil stain samples and Harshiyat source rock from a recent work of Hakimi et al. (2020) (modified after Huang & Meinschein, 1979), indicating a source rock containing mixed planktonic/bacterial organic matter and land plant input

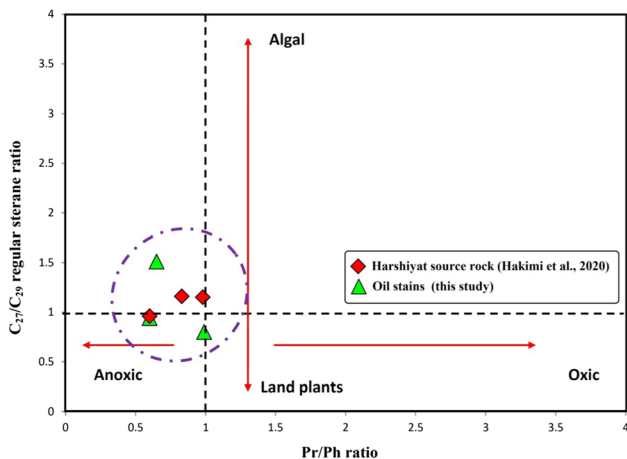


Fig. 11 Cross-plot for Pr/Ph versus the C_{27}/C_{29} regular sterane ratio, which further infers a mixed organic matter input

and CPI ratios were commonly used to estimate the order of thermal maturity [15, 46–51]. The high values of $22S/(22S + 22R)$ C_{32} hopane, Ts/Tm , $20S/(20S + 20R)$ and $\beta\beta/(\beta\beta + \alpha\alpha)$ C_{29} sterane ratios are indicative of a high thermal maturity level [47–50], whereas the relatively low CPIs and M_{30}/C_{30} ratios indicate a mature source rock [46, 51]. However, because the biomarker maturity parameters of Ts/Tm and CPI are influenced by the organic matter input [15, 51], it is insufficient to satisfy the thermal maturation criteria using CPI and Ts/Tm . Therefore, they must be used together with other biomarker ratios of aromatic and saturated fractions.

In this study, the most reliable biomarker ratios applied in determining maturity are $22S/(22S + 22R)$ of the C_{32} homohopane, M_{30}/C_{30} (Fig. 4a, and $20S/(20S + 20R)$ and $\beta\beta/(\beta\beta + \alpha\alpha)$ of the regular C_{29} steranes in the aliphatic hydrocarbon fraction [15, 46–49]. The aforementioned biomarker ratios apply over early maturity to peak maturity range, and the values increase as the degree of maturity increases [47–49].

The C_{32} homohopane ratio has been found applicable over the peak maturity range and reaches a maximum at 0.70 [49]. The analyzed oil stain samples have high values of C_{32} hopane ratio between 0.57 and 0.62 (Table 1), thus suggesting that the analyzed oil stain samples were generated from a mature source rock, equivalent early to peak maturity ($VR = 0.60$ – 80%). The different thermal maturity levels of the analyzed oil stain samples are also demonstrated by the C_{29} $20S/(20S + 20R)$ and $\beta\beta/(\beta\beta + \alpha\alpha)$ sterane ratios (Table 1). The C_{29} $20S/(20S + 20R)$ and $\beta\beta/(\beta\beta + \alpha\alpha)$ sterane ratios for three oil stain samples analyzed have relatively

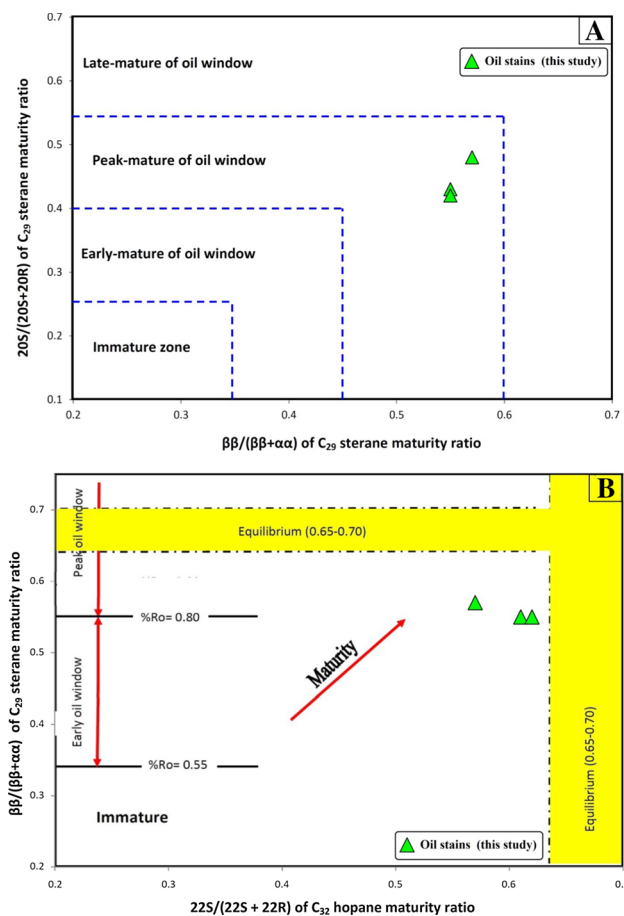


Fig. 12 Lipid biomarker maturity ratios of the C_{29} sterane $20S/(20S + 20R)$ and $\beta\beta/(\beta\beta + \alpha\alpha)$ and C_{32} hopane $22S/(22S + 22R)$, showing that two analyzed oil stain samples were generated from a mature source rock, equivalent to VR values between 0.55% and 0.80%

high values in the range of 0.42–0.48 and 0.55–0.57, respectively (Table 1), indicating a mature source rock, equivalent to moderate and peak maturity of oil window (Fig. 12a). The C_{32} hopane ratio values are also combined with the high C_{29} sterane $\beta\beta/(\beta\beta + \alpha\alpha)$ ratios (Table 1), further suggesting a mature source rock, consistent with VR of approximately 0.80% and more (Fig. 12b). In addition, the C_{30} moretane/ C_{30} hopane (M_{30}/C_{30}) ratio was also used to evaluate the thermal maturation of the analyzed oil stains and their probable source rock [46]. The presence of the relatively high C_{30} hopane compared to C_{30} moretane (Fig. 4a), with M_{30}/C_{30} ratio of less than 0.15 is indicative of a mature probable source rock as shown in the analyzed oil stain samples (Table 1), whereas the high M_{30}/C_{30} ratio of more than 0.20 indicate an immature source rock [46].

However, the sterane and hopane biomarkers were determined by the point of isomerization equilibrium values and input of organic matter [33, 47–49]. These saturated biomarker data alone should be used with caution because they are insufficient to satisfy all the thermal maturation criteria and should be supported by with other biomarker aromatic components. In this regard, aromatic maturity indicators of 2 oil stain samples analyzed (Table 1) are used to estimate the degree of thermal maturity of the probable source rock. The aromatic maturity parameters are typically based on the thermal stability of compounds as the quantity of the more stable isomer increases with maturity, whereas that of the less stable isomer decreases [20]. For example, the methyl-dibenzothiophene ratio (MDR) relies on the shift from the less stable 1-MDBT to the more stable 4-MDBT, and therefore, the parameter increases with thermal maturity [21]. According to the methyl-dibenzothiophene distributions, the MDR in the analyzed samples is estimated in the range of 1.80–4.19 (Table 1), indicating a mature source rock. Other aromatic parameters calculated for the analyzed samples include MPI-1 and MPI-2 shown in Table 1. The oil stain samples have relatively high values of MPI-1 and MPI-2 in the range of 0.72–0.82 and 0.89–1.02, respectively, suggesting a mature source rock (Fig. 13). However, the VRc values obtained from MPI-1 range from 0.83% to 0.89% (Table 1), consistent with a peak oil to mature oil windows [25], and further suggest that the analyzed oil stains were generated from a mature source rock.

4.5 Geochemical Correlations of Oil–Oil and Oil–Source Rock

The geochemistry of oil biomarkers and isotope compositions were used to classify the analyzed oil stain samples and then consequently identify possible oil–oil and oil–source rock correlations. In this regard, the geochemical genetic link of the oil samples themselves and their relationship with their potential source rock were demonstrated mainly from

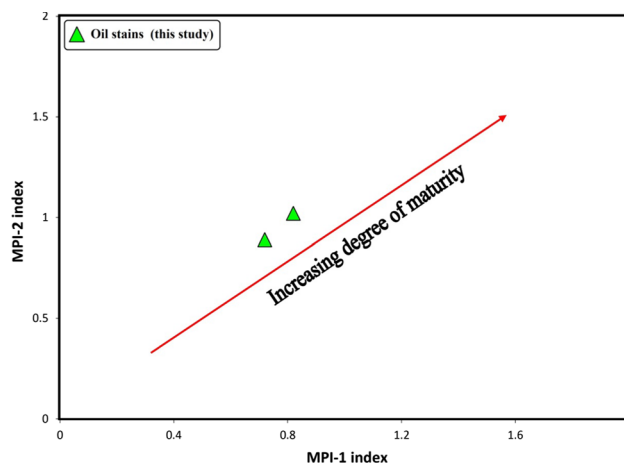


Fig. 13 Aromatic biomarker maturity indicators of methylphenanthrene (MPI-1 and MPI-2), further suggesting a mature source rock for the analyzed oil stain samples

the analytical results of the molecular biomarkers and $\delta^{13}C$ compositions of saturated and aromatic hydrocarbon fractions as discussed in the previous subsections. Accordingly, there is a positive oil–oil correlation. The analyzed oil stain samples are geochemically similar and are generally grouped into one oil family as demonstrated by the clustering of their molecular and isotopic characteristics (Figs. 5, 6, 7, 8, 9, 10, 11, 12, 13). These molecular and isotopic characteristics reveal that analyzed oil stain samples sourced from a clay-rich rock deposited in marine-reducing environmental conditions and likely contained mixed organic matter of planktonic, bacterial and land plant inputs (Figs. 5, 6, 7, 8, 9, 10, 11). The results of the saturated and aromatic maturity biomarkers further suggest that the analyzed oil stain samples are thermally mature and their source rock was at different maturity stages equivalent to a moderate to peak-mature oil window (Figs. 12 and 13).

The genetic relationship in term of oil–source rock correlation was also established based on the lipid biomarkers and their environmental biomarker indicators with geochemical isotopic results of the analyzed oil stain samples. The Harshiyat shale source rock from exploration well locations in the closed offshore Jiza-Qamar Basin was discussed in the recent published work of Hakimi et al. [2]. The Harshiyat shales in the well locations of the offshore Jiza-Qamar contain mixed organic matter of marine and terrestrial organic matter and were deposited under suboxic marine environmental conditions [2]. These characteristics of the Harshiyat shales are consistent with those of analyzed oil stains in this study as shown by the clustering of their ratios and parameters (Figs. 5, 6, 7, 8, 9, 10, 11). Based on the clustering of their molecular and isotopic characteristics, a positive oil–source rock correlation is evidenced and suggests that the analyzed oil stain samples were generated

from the Harshiyat shale source rock at sufficient maturity levels. Moreover, the $\delta^{13}C_{Sat}$ data suggest that the analyzed oil stain samples were sourced from the Cretaceous source rocks (Fig. 5b) and this is also consistent with the Late Cretaceous deposition time of the Harshiyat Formation (Fig. 2). Therefore, the shale intervals within the Late Cretaceous Harshiyat Formation are very likely source rocks for the analyzed oil stain samples.

As Hakimi et al. [2] reported that the analyzed Harshiyat shale samples from studied wells in the offshore Jiza-Qamar Basin

Basin were buried in a relatively shallower depth of less than 2400 m and reached an early mature stage of oil-generation window, equivalent to VR = 0.51%. Therefore, the mature Harshiyat shale rocks, with relatively high maturity of the peak oil window in the known deeper locations, are the most probable potential source rocks, where the Harshiyat source rock reached a high burial temperature depth of more than 3000 m as indicated by the 2D seismic section (Fig. 14). This finding is also supported by the geological situation of the Mahara Group, whereby the Mahara formations, including Harshiyat Formation, stratigraphically underlie the other formations in the offshore Jiza-Qamar Basin; therefore, the oils from Harshiyat shale source rock were very likely generated at a sufficient thermal burial depth in the offshore Jiza-Qamar Basin (Fig. 14). Before migration along vertical migration pathways through fault up to the shallow stratigraphic rocks in the Hadramaut High area is indicated by the cross section along the Hadramaut High and Jiza-Qamar Basin (Fig. 15).

5 Conclusions

This study discusses a combination of sterane and terpane biomarkers and $\delta^{13}C$ approaches to studying the saturated and aromatic hydrocarbon fractions in oil stains from five Harshiyat sandstone and carbonate rocks in the North Hadramaut High of eastern Yemen. The results are used to characterize the probable source rock of the studied oil stains samples, including the origin of the organic matter input, redox depositional conditions, lithology, and degree of thermal maturity. The following conclusions are derived from our organic geochemical results:

1. The biomarkers of the oil stain samples under study suggest a contribution of mixed marine planktonic/algae and terrestrial land plants from the clay-rich source rock

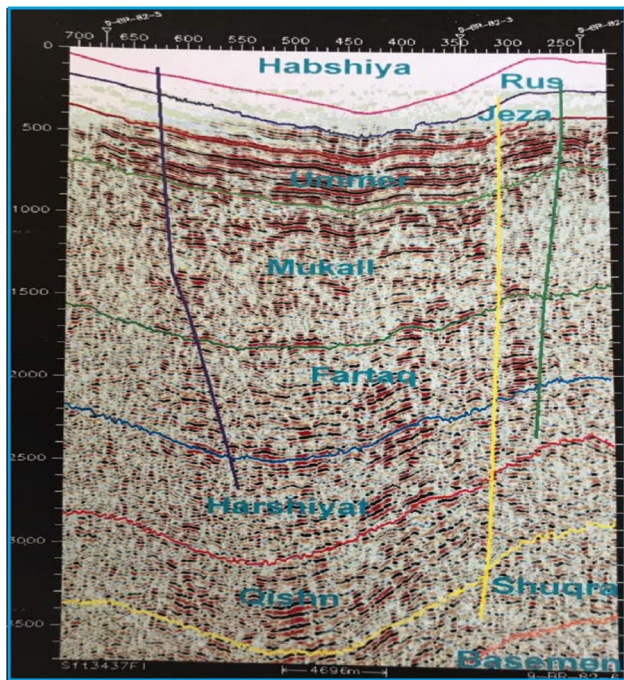


Fig. 14 Seismic cross section along offshore Jiza-Qamar Basin, showing the presence of the Harshiyat Formation in the known deeper locations, where the Harshiyat source rock reached a high burial temperature depth of more than 3000 m

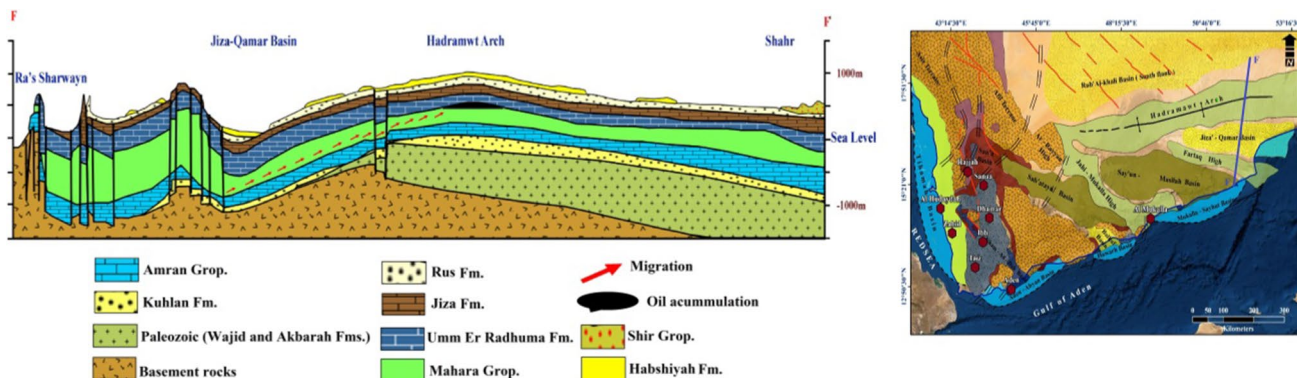


Fig. 15 Cross section shows the sedimentary successions and fault systems along the Ra's Sharwayn, offshore Jiza-Qamar Basin, North Hadramaut High area and Shahr (modified after Beydoun [52])

deposited in a marine environment under reducing conditions.

2. The $\delta^{13}\text{C}$ values of the saturated and aromatic hydrocarbon fractions further suggest a Cretaceous source rock that likely contained mixed marine and terrestrial organic matter.
3. Both sterane and terpane biomarkers and aromatic hydrocarbons suggest that the analyzed oil stain samples were generated from a mature source rock, corresponding to moderate and peak-mature oil windows.
4. The geochemical results of the biomarkers and $\delta^{13}\text{C}$ of the saturated and aromatic hydrocarbon fractions of the analyzed oil stain samples are similar and consistent with those of the shales within the Late Cretaceous Harshiyat Formation in the offshore Jiza-Qamar Basin. This conclusion further suggests a genetic link between the analyzed oil stain samples and the marine clay-rich source rock in the Late Cretaceous Harshiyat Formation.

Acknowledgements The first author is grateful to the Petroleum Exploration and Production Authority (PEPA), Republic of Yemen, for providing the geochemical data for this research. The authors extend their sincere appreciation to the Research Supporting Project number (RSP-2020/92), King Saud University, Riyadh, Saudi Arabia. We kindly acknowledged Prof. Dr. Bassam El Ali, Editor-in-Chief and subject Editor as well as two anonymous reviewers that helped us to improve the original manuscript.

References

1. Hakimi, M.H.; Ahmed, A.F.: Petroleum source rock characterization and hydrocarbon generation modeling of the Cretaceous sediments in the Jiza sub-basin, eastern Yemen. *Mar. Pet. Geol.* **75**, 356–373 (2016). <https://doi.org/10.1016/j.marpetgeo.2016.04.008>
2. Hakimi, M.H.; Ahmed, A.; Kahal, A.Y.; Hersi, O.S.; Al Faiji, H.J.; Qaysi, S.: Organic geochemistry and basin modeling of Late Cretaceous Harshiyat Formation in the onshore and offshore basins in Yemen: implications for effective source rock potential and hydrocarbon generation. *Mar. Pet. Geol.* (2020). <https://doi.org/10.1016/j.marpetgeo.2020.104701>
3. Beydoun, Z.R.; As-Saruri, M.A.L.; El-Nakhal, H.; Al-Ganad, I.N.; Baraba, R.S.; Nani, A.O.; Al-Aawah, M.H.: International lexicon of stratigraphy. Vol. III, Repub. Yemen, Second Ed. Int. union Geol. Sci. Minist. oil Miner. Resour. Repub. Yemen Publ. 34, 245 (1998)
4. As-Saruri, M.A.; Sorkhabi, R.; Baraba, R.: Sedimentary basins of Yemen: their tectonic development and lithostratigraphic cover. *Arab. J. Geosci.* **3**, 515–527 (2010). <https://doi.org/10.1007/s12517-010-0189-z>
5. Al Areeq, N.M.; Soliman, M.A.; Essa, M.A.; Al-Azazi, N.A.: Diagenesis and reservoir quality analysis in the Lower Cretaceous Qishn sandstones from Masila oilfields in the Sayun-Masila Basin, eastern Yemen. *Geol. J.* **51**, 405–420 (2016). <https://doi.org/10.1002/gj.2639>
6. Hakimi, M.H.; Shalaby, M.R.; Abdullah, W.H.: Diagenetic characteristics and reservoir quality of the Lower Cretaceous Biyadh sandstones at Kharir oilfield in the western central Masila Basin. *Yemen. J. Asian Earth Sci.* **51**, 109–120 (2012). <https://doi.org/10.1016/j.jseae.2012.03.004>
7. King, W.A.; Mills, B.R.; Gardiner, S.; Abdillahi, A.A.: The Masila fields, Republic of Yemen. In: AAPG Memoir. pp. 275–295 (2005)
8. Al-Wosabi, K.A.I. Alaug, A.S.: Calcareous nannofossils biostratigraphy of the Late Campanian–Early Maastrichtian Age, Block 16, Jiza-Qamar Basin, Eastern Yemen. *Arab. J. Geosci.* **6**, 3581–3594 (2013). <https://doi.org/10.1007/s12517-012-0642-2>
9. Hakimi, M.H.; Abdullah, W.H.: Source rock characteristics and hydrocarbon generation modelling of Upper Cretaceous Mukalla Formation in the Jiza-Qamar Basin Eastern Yemen. *Mar. Pet. Geol.* **51**, 100–116 (2014). <https://doi.org/10.1016/j.marpetgeo.2013.11.022>
10. Hakimi, M.H.; Abdullah, W.H.; Mustapha, K.A.; Adegoko, A.K.: Petroleum generation modeling of the Late Cretaceous coals from the Jiza-Qamar Basin as infer by kerogen pyrolysis and bulk kinetics. *Fuel* **154**, 24–34 (2015). <https://doi.org/10.1016/j.fuel.2015.03.055>
11. Hakimi, M.H.; Alaug, A.S.; Ahmed, A.F.; Yahya, M.M.A.; El Nady, M.M.; Ismail, I.M.: Simulating the timing of petroleum generation and expulsion from deltaic source rocks: implications for Late Cretaceous petroleum system in the offshore Jiza-Qamar Basin Eastern Yemen. *J. Pet. Sci. Eng.* **170**, 620–642 (2018). <https://doi.org/10.1016/j.petrol.2018.06.076>
12. Hakimi, M.H.; Ahmed, A.F.: Organic-geochemistry characterization of the Paleogene to Neogene source rocks in the Sayhut sub-basin, Gulf of Aden Basin, with emphasis on organicmatter input and petroleumgeneration potential. *Am. Assoc. Pet. Geol. Bull.* **100**, 1749–1774 (2016). <https://doi.org/10.1306/05241615201>
13. Arora, A.; Dutta, S.; Gogoi, B.; Banerjee, S.: The effects of igneous dike intrusion on organic geochemistry of black shale and its implications: late Jurassic Jhuran Formation. *India. Int. J. Coal Geol.* **178**, 84–99 (2017). <https://doi.org/10.1016/j.coal.2017.05.002>
14. Makeen, Y.M.; Abdullah, W.H.; Hakimi, M.H.: Biological markers and organic petrology study of organic matter in the Lower Cretaceous Abu Gabra sediments (Muglad Basin, Sudan): origin, type and palaeoenvironmental conditions. *Arab. J. Geosci.* **8**, 489–506 (2015). <https://doi.org/10.1007/s12517-013-1203-z>
15. Peters, K.E.; Walters, C.C.; Moldowan, J.M.: The biomarker guide: Biomarkers and isotopes in petroleum exploration and earth history, Vol. 2. Press Synd. Univ, Cambridge (2005)
16. Philp, R.P.: Biological markers in fossil fuel production. *Mass Spectrom. Rev.* **4**, 1–54 (1985). <https://doi.org/10.1002/mas.1280040102>
17. Powell, T.G.; McKirdy, D.M.: Relationship between ratio of pristane to phytane, crude oil composition and geological environment in Australia. *Nat. Phys. Sci.* **243**, 37–39 (1973). <https://doi.org/10.1038/physci243037a0>
18. Gürgey, K.: Geochemical characteristics and thermal maturity of oils from the thrace basin (western Turkey) and western Turkmenistan. *J. Pet. Geol.* **22**, 167–189 (1999). <https://doi.org/10.1111/j.1747-5457.1999.tb00466.x>
19. Chakhmakhchev, A.; Suzuki, N.: Aromatic sulfur compounds as maturity indicators for petroleum from the Buzuluk depression. *Russia. Org. Geochem.* **23**, 617–625 (1995). [https://doi.org/10.1016/0146-6380\(95\)00050-0](https://doi.org/10.1016/0146-6380(95)00050-0)
20. Chakhmakhchev, A.; Suzuki, M.; Takayama, K.: Distribution of alkylated dibenzothiophenes in petroleum as a tool for maturity assessments. *Org. Geochem.* **26**, 483–489 (1997). [https://doi.org/10.1016/S0146-6380\(97\)00022-3](https://doi.org/10.1016/S0146-6380(97)00022-3)
21. Radke, M.; Welte, D.H.; Willsch, H.: Maturity parameters based on aromatic hydrocarbons: influence of the organic matter type. *Org. Geochem.* **10**, 51–63 (1986). [https://doi.org/10.1016/0146-6380\(86\)90008-2](https://doi.org/10.1016/0146-6380(86)90008-2)



22. Hughes, W.B.; Holba, A.G.; Dzou, L.I.P.: The ratios of dibenzothiophene to phenanthrene and pristane to phytane as indicators of depositional environment and lithology of petroleum source rocks. *Geochim. Cosmochim. Acta.* **59**, 3581–3598 (1995). [https://doi.org/10.1016/0016-7037\(95\)00225-O](https://doi.org/10.1016/0016-7037(95)00225-O)
23. Asif, M.; Wenger, L.M.: Heterocyclic aromatic hydrocarbon distributions in petroleum: a source facies assessment tool. *Org. Geochem.* (2019). <https://doi.org/10.1016/j.orggeochem.2019.07.005>
24. Radke, M.; Vriend, S.P.; Ramanampisoa, L.R.: Alkyldibenzofurans in terrestrial rocks: influence of organic facies and maturation. *Geochim. Cosmochim. Acta.* **64**, 275–286 (2000). [https://doi.org/10.1016/S0016-7037\(99\)00287-2](https://doi.org/10.1016/S0016-7037(99)00287-2)
25. Radke, M.; Welte, D.H.: The methylphenanthrene index (MPI): a maturity parameter based on aromatic hydrocarbons. *Adv. Org. Geochem.* **1981**, 504–512 (1983)
26. Collister, J.W.; Wavrek, D.A.: $\delta^{13}\text{C}$ Compositions of saturate and aromatic fractions of lacustrine oils and bitumens: evidence for water column stratification. *Org. Geochem.* **24**, 913–920 (1996). [https://doi.org/10.1016/S0146-6380\(96\)00066-6](https://doi.org/10.1016/S0146-6380(96)00066-6)
27. Boreham, C.; Hope, J.; Hartung-Kagi, B.: Understanding source, distribution and preservation of Australian natural gas: a geochemical perspective. *APPEA J.* **41**, 523 (2001). <https://doi.org/10.1071/aj00026>
28. Sofer, Z.: Stable carbon isotope compositions of crude oils: application to source depositional environments and petroleum alteration. *Am. Assoc. Pet. Geol. Bull.* **68**, 31–49 (1984). <https://doi.org/10.1306/ad460963-16f7-11d7-8645000102c1865d>
29. Summons, R.E.; Thomas, J.; Maxwell, J.R.; Boreham, C.J.: Secular and environmental constraints on the occurrence of dinosterane in sediments. *Geochim. Cosmochim. Acta.* **56**, 2437–2444 (1992). [https://doi.org/10.1016/0016-7037\(92\)90200-3](https://doi.org/10.1016/0016-7037(92)90200-3)
30. Jasper, J.P.; Gagosian, R.B.: The sources and deposition of organic matter in the late quaternary pigmy basin Gulf of Mexico. *Geochim. Cosmochim. Acta.* **54**, 1117–1132 (1990). [https://doi.org/10.1016/0016-7037\(90\)90443-O](https://doi.org/10.1016/0016-7037(90)90443-O)
31. Andrusevich, V.E.; Engel, M.H.; Zumberge, J.E.; Brothers, L.A.: Secular, episodic changes in stable carbon isotope composition of crude oils. *Chem. Geol.* **152**, 59–72 (1998). [https://doi.org/10.1016/S0009-2541\(98\)00096-5](https://doi.org/10.1016/S0009-2541(98)00096-5)
32. Hakimi, M.H.; Abdullah, W.H.: Organic geochemical characteristics and oil generating potential of the upper jurassic safer shale sediments in the Marib-Shabowah Basin, western Yemen. *Org. Geochem.* **54**, 115–124 (2013). <https://doi.org/10.1016/j.orggeochem.2012.10.003>
33. Peters, K.E.; Moldowan, J.M.: The biomarker guide: interpreting molecular fossils in petroleum and ancient sediments. (1993)
34. Connan, J.; Bouroulllec, J.; Dessort, D.; Albrecht, P.: The microbial input in carbonate-anhydrite facies of a sabkha palaeoenvironment from Guatemala: a molecular approach. *Org. Geochem.* **10**, 29–50 (1986). [https://doi.org/10.1016/0146-6380\(86\)90007-0](https://doi.org/10.1016/0146-6380(86)90007-0)
35. Moldowan, J.M.; Sundararaman, P.; Schoell, M.: Sensitivity of biomarker properties to depositional environment and/or source input in the Lower Toarcian of SW-Germany. *Org. Geochem.* **10**, 915–926 (1986). [https://doi.org/10.1016/S0146-6380\(86\)80029-8](https://doi.org/10.1016/S0146-6380(86)80029-8)
36. Tissot, B.P.; Welte, D.H.: Production and Accumulation of Organic Matter The Organic Carbon Cycle. In: *Petroleum Formation and Occurrence*. pp. 3–13. Springer Berlin Heidelberg (1984)
37. Alias, F.L.; Abdullah, W.H.; Hakimi, M.H.; Azhar, M.H.; Kugler, R.L.: Organic geochemical characteristics and depositional environment of the Tertiary Tanjong Formation coals in the Pinangah area, onshore Sabah, Malaysia. *Int. J. Coal Geol.* **104**, 9–21 (2012). <https://doi.org/10.1016/j.coal.2012.09.005>
38. Sarki Yandoka, B.M.; Abdullah, W.H.; Abubakar, M.B.; Hakimi, M.H.; Mustapha, K.A.; Adegoke, A.K.: Organic geochemical characteristics of Cretaceous Lamja Formation from Yola Sub-basin, Northern Benue Trough, NE Nigeria: implication for hydrocarbon-generating potential and paleodepositional setting. *Arab. J. Geosci.* **8**, 7371–7386 (2015). <https://doi.org/10.1007/s12517-014-1713-3>
39. de Aquino Neto, F.R.: Occurrence and formation of tricyclic and tetracyclic terpanes in sediments and petroleum. *Adv. Org. geochemistry* **1981**, 659–667 (1983)
40. Aquino Neto, F.R.; Trigu is, J., Azevedo, DA, Rodrigues, R., Simoneit, BRT, : Organic geochemistry of geologically unrelated tasmanites. *Org. Geochem.* **18**, 791–803 (1992)
41. Hanson, A.D.; Zhang, S.C.; Moldowan, J.M.; Liang, D.G.; Zhang, B.M.: Molecular organic geochemistry of the Tarim basin, Northwest China. *Am. Assoc. Pet. Geol. Bull.* **84**, 1109–1128 (2000). <https://doi.org/10.1306/a9673c52-1738-11d7-8645000102c1865d>
42. Marynowski, L.; Narkiewicz, M.; Grelowski, C.: Biomarkers as environmental indicators in a carbonate complex, example from the Middle to Upper Devonian, Holy Cross mountains, Poland. *Sediment. Geol.* **137**, 187–212 (2000). [https://doi.org/10.1016/S0037-0738\(00\)00157-3](https://doi.org/10.1016/S0037-0738(00)00157-3)
43. Volk, H.; George, S.C.; Middleton, H.; Schofield, S.: Geochemical comparison of fluid inclusion and present-day oil accumulations in the Papuan Foreland-Evidence for previously unrecognised petroleum source rocks. *Org. Geochem.* **36**, 29–51 (2005). <https://doi.org/10.1016/j.orggeochem.2004.07.018>
44. Zumberge, J.E.: Terpenoid biomarker distributions in low maturity crude oils. *Org. Geochem.* **11**, 479–496 (1987). [https://doi.org/10.1016/0146-6380\(87\)90004-0](https://doi.org/10.1016/0146-6380(87)90004-0)
45. Huang, W.Y.; Meinschein, W.G.: Sterols as ecological indicators. *Geochim. Cosmochim. Acta.* **43**, 739–745 (1979). [https://doi.org/10.1016/0016-7037\(79\)90257-6](https://doi.org/10.1016/0016-7037(79)90257-6)
46. Mackenzie, A.S.; Patience, R.L.; Maxwell, J.R.; Durand, B.; Vandenbrouke, M.: Molecular parameters for the maturation of sedimentary organic matter of the Toarcian Shales, Paris Basin France. *Geochim. cosmochim. Acta* **44**, 1709–1721 (1980)
47. Seifert, W.K.; Michael Moldowan, J.: Applications of steranes, terpanes and monoaromatics to the maturation, migration and source of crude oils. *Geochim. Cosmochim. Acta.* **42**, 77–95 (1978). [https://doi.org/10.1016/0016-7037\(78\)90219-3](https://doi.org/10.1016/0016-7037(78)90219-3)
48. Seifert, W.K.; Moldowan, J.M.: Paleoreconstruction by biological markers. *Geochim. Cosmochim. Acta.* **45**, 783–794 (1981). [https://doi.org/10.1016/0016-7037\(81\)90108-3](https://doi.org/10.1016/0016-7037(81)90108-3)
49. Seifert, W.K.; Moldowan, J.M.: Use of biological markers in petroleum exploration. *Methods geochemistry Geophys.* **24**, 261–290 (1986)
50. El. Nady, M.M.; Harb, F.M.; Mohamed, N.S.: Biomarker characteristics of crude oils from Ashrafi and GH oilfields in the Gulf of Suez, Egypt: An implication to source input and paleoenvironmental assessments. *Egypt. J. Pet.* **23**, 455–459 (2014). <https://doi.org/10.1016/j.ejpe.2014.11.002>
51. Bray, E.E.; Evans, E.D.: Distribution of n-paraffins as a clue to recognition of source beds. *Geochim. Cosmochim. Acta.* **22**, 2–15 (1961). [https://doi.org/10.1016/0016-7037\(61\)90069-2](https://doi.org/10.1016/0016-7037(61)90069-2)
52. Beydoun, Z.R.: Geology of the Arabian Peninsula; Eastern Aden Protectorate and Part of Dhufar. (1966)

